

VOLUME 37 NUMBER 7
JULY 2019

ISSN: 1002-0721
CODEN JREAE 6

Journal of **Rare Earths**



万方数据



CONTENTS

INVITED REVIEW

Recent developments and progress of inorganic photo-stimulated phosphors

.....Xiaotong Fan, Zhichao Liu, Xiuxia Yang, Wenbo Chen, Wei Zeng, Shuyu Tian, Xue Yu, Jianbei Qiu, Xuhui Xu 679

SPECTROSCOPY, LUMINESCENCE AND PHOSPHORS

Sub-10 nm lanthanide-doped SrFCl nanoplates: Controlled synthesis, optical properties and bioimaging

.....Jiaojiao Wei, Wei Lian, Wei Zheng, Xiaoying Shang, Meiran Zhang, Tao Dai, Xueyuan Chen 691

Rational design of monovalent ions (Li, Na, K) co-doped $\text{ZnAl}_2\text{O}_4\text{:Eu}^{3+}$ nanocrystals enabling versatile robust latentfingerprint visualizationF. Femila Komahal, H. Nagabhushana, R.B. Basavaraj, G.P. Darshan,
Hajeebaba K. Inamdar, S.C. Sharma, B. Daruka Prasad 699

RARE EARTH CATALYSIS

Effect of PdO_x structure properties on catalytic performance of $\text{Pd/Ce}_{0.67}\text{Zr}_{0.33}\text{O}_2$ catalyst for CO, HC and NO_x elimination

.....Ting Wang, Xiaolin Guo, Siyu Lin, Renxian Zhou 706

 Al_2O_3 supported hybrid Pd– CeO_2 colloidal spheres and its enhanced catalytic performances for methane combustion

.....Xinwei Yang, Chenhao Du, Yanglong Guo, Yun Guo, Li Wang, Yunsong Wang, Wangcheng Zhan 714

Catalytic performance of Zr-doped CuO– CeO_2 oxides for CO selective oxidation in H_2 -rich stream

.....Limin Shi, Chuanlei Gao, Fenghai Guo, Yujing Wang, Tiebang Zhang 720

Preparation of Ce^{3+} doped Bi_2O_3 hollow needle-shape with enhanced visible-light photocatalytic activity

.....Wenwen Zhang, Shaomin Gao, Donghui Chen 726

MAGNETISM AND MAGNETIC MATERIALS

Morphology and magnetic traits of strontium nanohexaferrites: Effects of manganese/yttrium co-substitution

.....M.A. Almessiere, Y. Slimani, H.S. El Sayed, A. Baykal 732

ADVANCED RARE EARTH MATERIALS

New environmental-friendly yellow pigments $\text{Y}_{4-x}\text{A}_x\text{MoO}_{9+\delta}$ (A=Ta, Tb)

.....Mengjun Cai, Shuai Feng Chen, Xinsheng Ma, Jianding Chen 741

Gaseous hydrogen storage properties of Mg-Y-Ni-Cu alloys prepared by melt spinning

.....Yanghuan Zhang, Yaqin Li, Wei Zhang, Zeming Yuan, Zhonghui Hou, Yan Qi, Shihai Guo 750

CHEMISTRY AND HYDROMETALLURGY

Decomposition process of bastnaesite concentrate in NaOH–CaO– H_2O system

.....Jiang Liu, Ting'an Zhang, Zhihe Dou, Yan Liu, Guozhi Lv 760

RARE EARTH APPLICATIONS

Phase separation and crystallization of La_2O_3 doped $\text{ZnO-B}_2\text{O}_3\text{-SiO}_2$ glass

.....Mitang Wang, Long Fang, Mei Li, Zhaogang Liu, Yanhong Hu, Xiaowei Zhang, Wei Deng, Ruhil Dongol 767

Adhesion at cerium doped metal-ceramic $\alpha\text{-Fe/WC}$ interface: A first-principles calculation

.....Guiying Yang, Yan Liu, Zongqiu Hang, Naiyuan Xi, Hao Fu, Hui Chen 773

Lanthanum chloride improves maize grain yield by promoting photosynthetic characteristics, antioxidants enzymes and

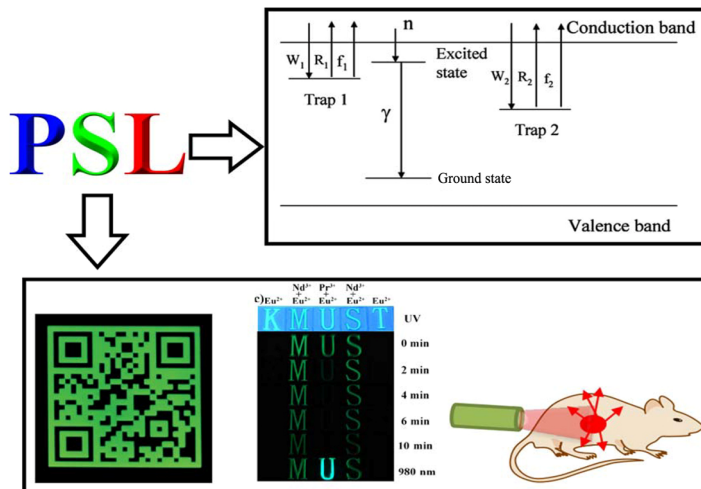
endogenous hormone at reproductive stagesWenwen Cui, Muhammad Kamran, Quanhao Song, Bingyun Zuo,
Zhikuan Jia, Qingfang Han 781

CONTENTS

INVITED REVIEW

- 679 Recent developments and progress of inorganic photo-stimulated phosphors

Xiaotong Fan, Zhichao Liu, Xiuxia Yang,
Wenbo Chen, Wei Zeng, Shuyu Tian, Xue Yu,
Jianbei Qiu, Xuhui Xu



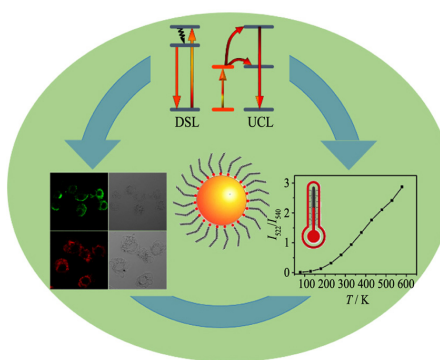
The review is devoted to introducing the applications and mechanism of photo-stimulated phosphors

J. Rare Earths, (37) 2019: 679-690

SPECTROSCOPY, LUMINESCENCE AND PHOSPHORS

- 691 Sub-10 nm lanthanide-doped SrFCl nanoprobe: Controlled synthesis, optical properties and bioimaging

Jiaojiao Wei, Wei Lian, Wei Zheng,
Xiaoying Shang, Meiran Zhang, Tao Dai,
Xueyuan Chen

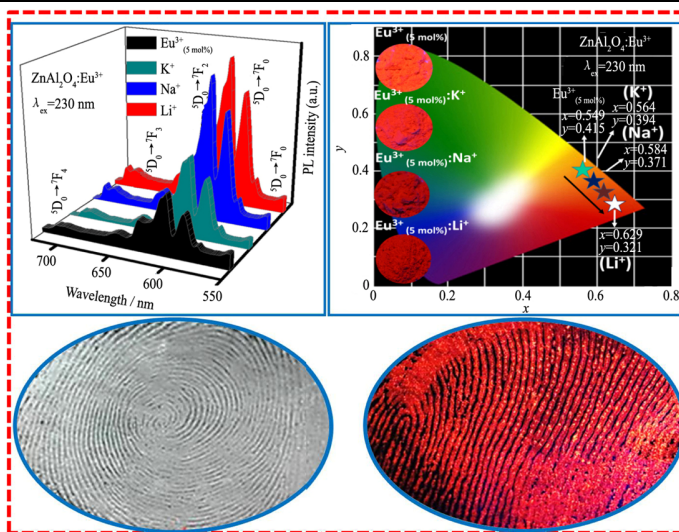


We developed a novel hot-injection method for synthesizing sub-10 nm lanthanide-doped SrFCl nanocrystals with efficient upconverting and downshifting luminescence and demonstrate their potential applications as sensitive luminescent nanoprobe for targeted cancer cell imaging and non-contact thermal sensing

J. Rare Earths, (37) 2019: 691-698

- 699 Rational design of monovalent ions (Li, Na, K) co-doped $\text{ZnAl}_2\text{O}_4:\text{Eu}^{3+}$ nanocrystals enabling versatile robust latent fingerprint visualization

F. Femila Komahal, H. Nagabhushana,
R.B. Basavaraj, G.P. Darshan,
Hajeebaba K. Inamdar, S.C. Sharma,
B. Daruka Prasad

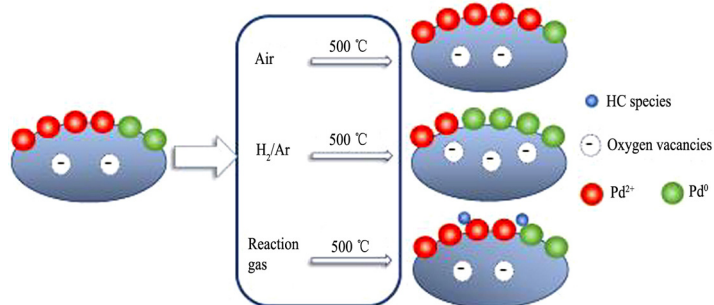


Alkali metal ions ($\text{M}^+ = \text{Na}, \text{Li}, \text{K}$) co-doped $\text{ZnAl}_2\text{O}_4:\text{Eu}^{3+}$ (5 mol %) (ZAE) nanopowders (NPs) were prepared via solution combustion route using *mimosapudica* (MP) leaves extract as a fuel. A 2-fold enhancement in PL intensity was observed in Li^+ co-doped samples. The optimized $\text{ZnAl}_2\text{O}_4:\text{Eu}^{3+}$ (5 mol %), Li^+ (1 wt %) (ZAE) NPs were used to visualize LFPs on various porous, semi-porous and non-porous surfaces through robust powder dusting technique

J. Rare Earths, (37) 2019: 699-705

- 706 Effect of PdO_x structure properties on catalytic performance of $\text{Pd/Ce}_{0.67}\text{Zr}_{0.33}\text{O}_2$ catalyst for CO, HC and NO_x elimination

Ting Wang, Xiaolin Guo, Siyu Lin,
Renxian Zhou

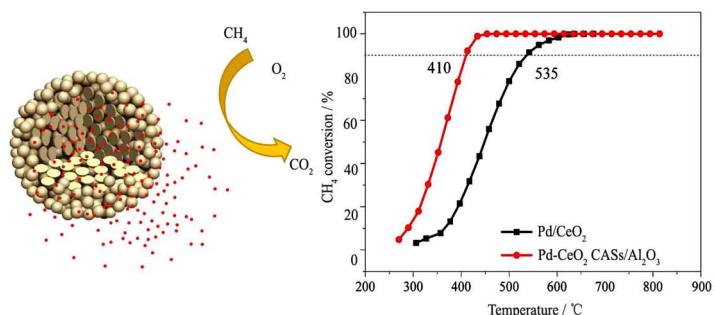


The variation in catalytic performances of $\text{Pd/Ce}_{0.67}\text{Zr}_{0.33}\text{O}_2$ catalyst for CO, HC and NO_x elimination by the pretreatment atmosphere is revealed

J. Rare Earths, (37) 2019: 706-713

- 714 Al_2O_3 supported hybrid Pd– CeO_2 colloidal spheres and its enhanced catalytic performances for methane combustion

Xinwei Yang, Chenhao Du, Yanglong Guo,
Yun Guo, Li Wang, Yunsong Wang,
Wangcheng Zhan

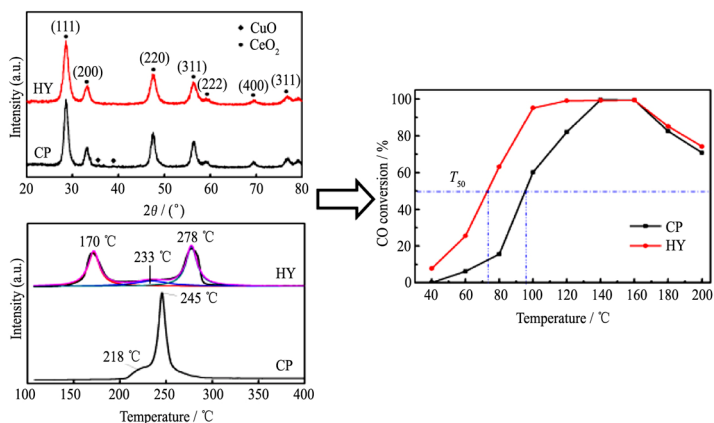


Ordered hybrid Pd– CeO_2 colloidal assembled spheres (CASs) with highly dispersed Pd clusters were synthesized. Pd– CeO_2 CASs supported on $\gamma\text{-Al}_2\text{O}_3$ show high catalytic performance and thermal stability in methane combustion. The enhanced catalytic activity can be attributed to the more number of catalytically active Pd–O–Ce sites

J. Rare Earths, (37) 2019: 714-719

- 720 Catalytic performance of Zr-doped CuO-CeO_2 oxides for CO selective oxidation in H_2 -rich stream

Limin Shi, Chuanlei Gao, Fenghai Guo,
Yujing Wang, Tiebang Zhang



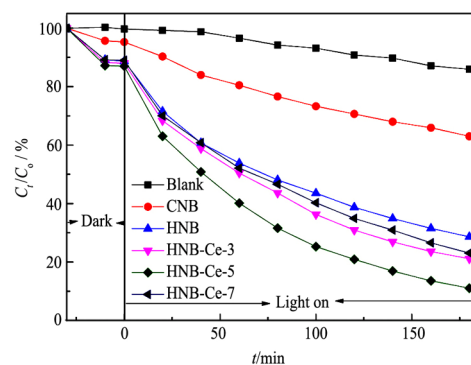
Hydrothermal method prepared $\text{CuO-CeO}_2\text{-ZrO}_2$ catalyst preserves small crystalline size, high dispersion of active components and high reducibility. Meanwhile, the presence of more CO oxidation sites on the surface and the formation of more Cu^+ species and oxygen vacancies on the copper-ceria interface account for its superior low-temperature activity and CO_2 selectivity, compared with those of the catalyst prepared by coprecipitation

J. Rare Earths, (37) 2019: 720-725

- 726 Preparation of Ce^{3+} doped Bi_2O_3 hollow needle-shape with enhanced visible-light photocatalytic activity

Wenwen Zhang, Shaomin Gao, Donghui Chen

J. Rare Earths, (37) 2019: 726-731



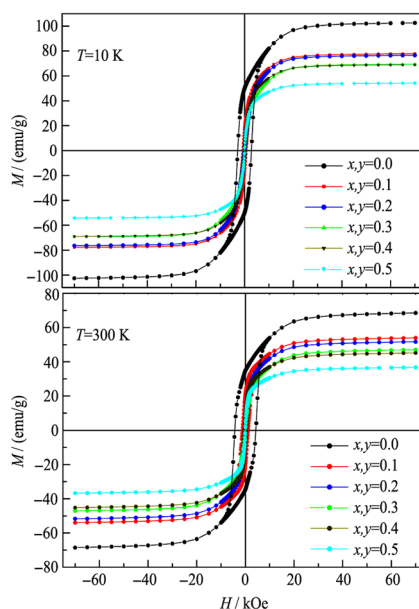
Photodegradation efficiency curves of CNB, HNB and HNB-Ce. As lighting on, the concentration of TC was decreasing over time. 3 h later, all the samples doped with Ce^{3+} exhibit better photocatalytic property than that of undoped Bi_2O_3 for the photodegradation of TC, which indicates that the doped of Ce^{3+} is an efficient method for enhancing the photocatalysis of Bi_2O_3 . However, the improved performance is also dependent on the amount of doped Ce. 5 wt% Ce doping shows the optimum activity

MAGNETISM AND MAGNETIC MATERIALS

- 732 Morphology and magnetic traits of strontium nanohexaferrites: Effects of manganese/yttrium co-substitution

M.A. Almessiere, Y. Slimani, H.S. El Sayed, A. Baykal

J. Rare Earths, (37) 2019: 732-740

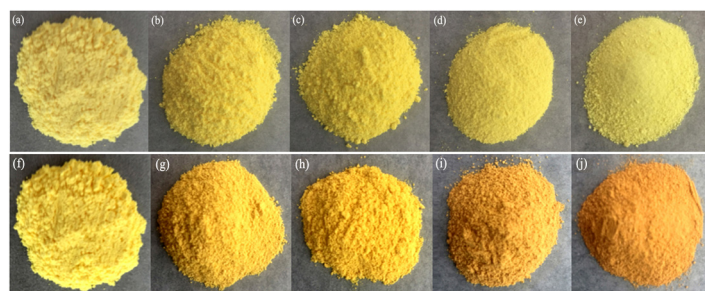


The influence of manganese (Mn) and yttrium (Y) co-substitution on the microstructural, morphological and magnetic properties of strontium nanohexaferrites ($\text{Sr}_{1-x}\text{Mn}_x\text{Fe}_{12-y}\text{Y}_y\text{O}_{19}$; $0.0 \leq x=y \leq 0.5$) was examined. The magnetic hysteresis loops of the various produced nanohexaferrites indicate ferrimagnetic behavior

ADVANCED RARE EARTH MATERIALS

- 741 New environmental-friendly yellow pigments $\text{Y}_{4-x}\text{A}_x\text{MoO}_{9+\delta}$ (A=Ta, Tb)

Mengjun Cai, Shuai Feng Chen, Xinsheng Ma, Jianding Chen



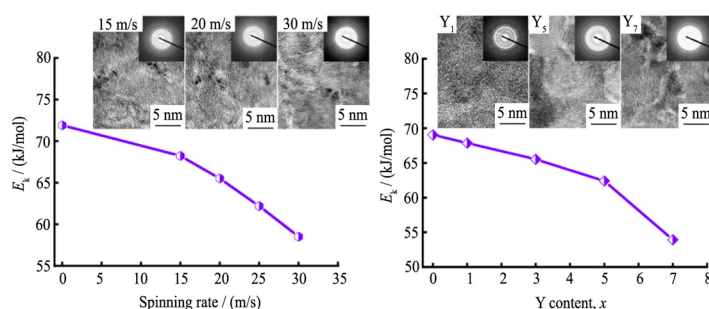
A series of environmental-friendly yellow pigments $\text{Y}_{4-x}\text{A}_x\text{MoO}_{9+\delta}$ (A=Ta, Tb) were successfully synthesized. The typical pigment $\text{Y}_{3.9}\text{Ta}_{0.1}\text{MoO}_{9+\delta}$ is of tiptop colorant values with $L^* = 91.7$, $a^* = -3.8$, $b^* = 59.8$ due to the substitution of Ta^{5+} for Y^{3+} in Y_4MoO_9 . The typical pigment $\text{Y}_{3.99}\text{Tb}_{0.01}\text{MoO}_{9+\delta}$ is of superior colorant values with $L^* = 84.2$, $a^* = 1.8$, $b^* = 52.7$ due to the substitution of Tb^{3+} for Y^{3+} in Y_4MoO_9 .

- (a) $\text{Y}_4\text{MoO}_{9+\delta}$; (b) $\text{Y}_{3.95}\text{Ta}_{0.05}\text{MoO}_{9+\delta}$; (c) $\text{Y}_{3.9}\text{Ta}_{0.1}\text{MoO}_{9+\delta}$; (d) $\text{Y}_{3.8}\text{Ta}_{0.2}\text{MoO}_{9+\delta}$; (e) $\text{Y}_{3.6}\text{Ta}_{0.4}\text{MoO}_{9+\delta}$; (f) $\text{Y}_4\text{MoO}_{9+\delta}$; (g) $\text{Y}_{3.995}\text{Tb}_{0.005}\text{MoO}_{9+\delta}$; (h) $\text{Y}_{3.99}\text{Tb}_{0.01}\text{MoO}_{9+\delta}$; (i) $\text{Y}_{3.97}\text{Tb}_{0.03}\text{MoO}_{9+\delta}$; (j) $\text{Y}_{3.95}\text{Tb}_{0.05}\text{MoO}_{9+\delta}$

J. Rare Earths, (37) 2019: 741-749

- 750 Gaseous hydrogen storage properties of Mg-Y-Ni-Cu alloys prepared by melt spinning

Yanghuan Zhang, Yaqin Li, Wei Zhang,
Zeming Yuan, Zhonghui Hou, Yan Qi,
Shihai Guo



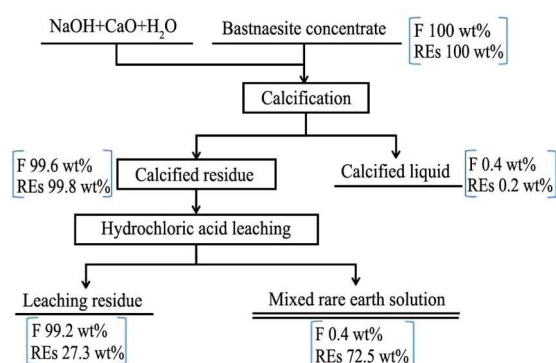
With the increase of spinning rate and Y content, amorphous phase increases and dehydrogenation activation energy decreases

J. Rare Earths, (37) 2019: 750-759

CHEMISTRY AND HYDROMETALLURGY

- 760 Decomposition process of bastnaesite concentrate in NaOH-CaO-H₂O system

Jiang Liu, Ting'an Zhang, Zhihe Dou,
Yan Liu, Guozhi Lv



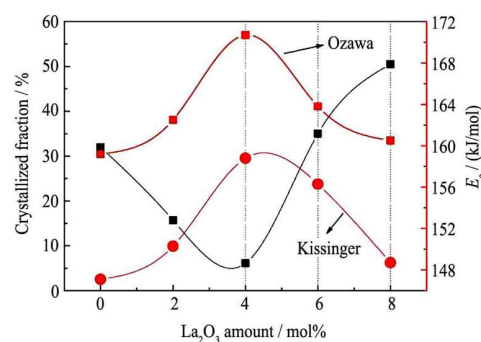
The calcification-leaching of bastnaesite concentrate was studied. Firstly bastnaesite is decomposed by calcification where REs and F are transformed into RE(OH)₃ and CaF₂, respectively and both concentrate in calcified residue. Then by HCl leaching, REs and F are separated. In final, 99.2 wt% of fluorine leaves in leaching residue and 72.5 wt% of REs are leached out

J. Rare Earths, (37) 2019: 760-766

RARE EARTH APPLICATIONS

- 767 Phase separation and crystallization of La₂O₃ doped ZnO-B₂O₃-SiO₂ glass

Mitang Wang, Long Fang, Mei Li,
Zhaogang Liu, Yanhong Hu, Xiaowei Zhang,
Wei Deng, Ruhil Dongol

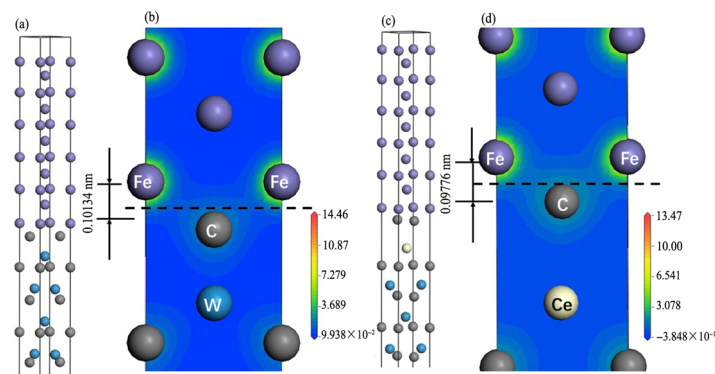


The dependence of the crystallization activation energy E_c of 60ZnO-30B₂O₃-10SiO₂ glass on the La₂O₃ doping amount is illustrated in the figure, the change trend of E_c values estimated by Ozawa and Kissinger methods is the same, as the doping amount of La₂O₃ increases from 0 to 8 mol%, the maximum value of crystallization activation energy E_c appears at 4 mol% of La₂O₃, indicating that the crystallization barrier needing to overcome is the largest for the glass doped with 4 mol% La₂O₃, as a result, the crystallization of glass is inhibited. This result can be used to control the depth of crystal layer on glass surface, crystallinity and thermal stability of 60ZnO-30B₂O₃-10SiO₂ glass by doping with different contents of La₂O₃

J. Rare Earths, (37) 2019: 767-772

773 Adhesion at cerium doped metal-ceramic α -Fe/WC interface: A first-principles calculation

Guiying Yang, Yan Liu, Zongqiu Hang,
Naiyuan Xi, Hao Fu, Hui Chen

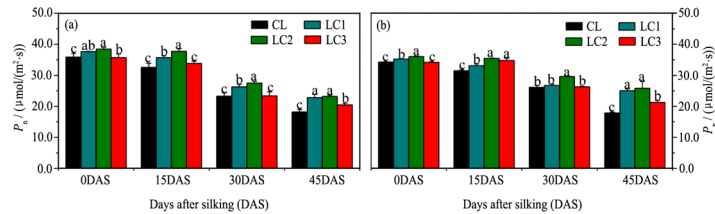


Compared with the un-doped coating interface ($W_{ad}=8.76 \text{ J/m}^2$, $d_0=0.10134 \text{ nm}$), the doped coating interface has a smaller interface distance ($d_0=0.09776 \text{ nm}$) and a larger interface binding energy ($W_{ad}=8.98 \text{ J/m}^2$). The interface charge distribution shows covalent and ionic bonding at the interface, which indicates that the doped interface is more stable

J. Rare Earths, (37) 2019: 773-780

781 Lanthanum chloride improves maize grain yield by promoting photosynthetic characteristics, antioxidants enzymes and endogenous hormone at reproductive stages

Wenwen Cui, Muhammad Kamran,
Quanhao Song, Bingyun Zuo, Zhikuan Jia,
Qingfang Han



Seed priming with LaCl_3 at 400 and 800 $\mu\text{mol/L}$ increase photosynthetic capacity of maize, while LC3 treatment has no significant effect on photosynthetic capacity in maize leaves

J. Rare Earths, (37) 2019: 781-790